# Assessment of radiative heat transfer impact on a temperature distribution inside a real industrial swirled furnace

(MRRFEU-KK.01.1.1.04.0070) Jurić, Filip; Vujanović, Milan; Živić, Marija; Holik, Mario; Wang, Xuebin; Duić, Neven

# ASSESSMENT OF RADIATIVE HEAT TRANSFER IMPACT ON A TEMPERATURE DISTRIBUTION INSIDE A REAL INDUSTRIAL SWIRLED FURNACE

by

## *Filip JURIĆ[a], Milan VUJANOVIĆ[a*], Marija ŽIVIĆ[b], Mario HOLIK[b], Xuebin WANG[c], and Neven DUIĆ[a]*

[a]Faculty of Mechanical Engineering and Naval Architecture, University of Zagreb, Zagreb, Croatia;
[b]Mechanical Engineering Faculty, Josip Juraj Strossmayer University of Osijek, Slavonski Brod, Croatia
[c]MOE Key Laboratory of Thermo-Fluid Science and Engineering, Xi'an Jiaotong University,
Xi'an, Shaanxi, China

*Combustion systems will continue to share a portion in energy sectors along the current energy transition, and therefore the attention is still given to the further improvements of their energy efficiency. Modern research and development processes of combustion systems are improbable without the usage of predictive numerical tools such as CFD. The radiative heat transfer in participating media is modelled in this work with discrete transfer radiative method (DTRM) and discrete ordinates method (DOM) by finite volume discretisation, in order to predict heat transfer inside combustion chamber accurately. The DTRM trace the rays in different directions from each face of the generated mesh. At the same time, DOM is described with the angle discretisation, where for each spatial angle the radiative transport equation needs to be solved. In combination with the steady combustion model in AVL FIRE™ CFD code, both models are applied for computation of temperature distribution in a real oil-fired industrial furnace for which the experimental results are available. For calculation of the absorption coefficient in both models weighted sum of grey gasses model is used. The focus of this work is to estimate radiative heat transfer with DTRM and DOM models and to validate obtained results against experimental data and calculations without radiative heat transfer, where approximately 25% higher temperatures are achieved. The validation results showed good agreement with the experimental data with a better prediction of the DOM model in the temperature trend near the furnace outlet. Both radiation modelling approaches show capability for the computation of radiative heat transfer in participating media on a complex validation case of the combustion process in oil-fired furnace.*

Keywords: *radiative heat transfer, participating media, furnace,
radiative absorption, combustion*

## Introduction

It is known that the radiative heat transfer as a fundamental heat transfer mechanism is not negligible in the overall heat transfer of the energy systems that work at the high tem-

---

[*]Corresponding author, e-mail: milan.vujanovic@fsb.hr

3664

Jurić, F., *et al.*: Assessment of Radiative Heat Transfer Impact …
THERMAL SCIENCE: Year 2020, Vol. 24, No. 6A, pp. 3663-3672

perature conditions. Recent researches show that if emissions concentrations are to be calculated, it is not enough to exclude the impact of radiation on overall heat transfer and consequently, on emission formation [1]. In numerical modelling of engineering systems that operate at high temperatures such as furnaces, boilers, jet engines and internal combustion engines the consideration of radiative heat transfer in calculations significantly influence the energy efficiency [2]. As one of the predictive tools in energy efficiency investigation, the CFD is frequently utilised for the research of combustion system designs to evaluate the heat transfer impact on their energy efficiency [3]. With the development of the computational resources, the radiative heat transfer models within CFD are commonly applied to evaluate the impact of the radiative heat transfer impact on total heat transfer and temperature distribution [4]. For the calculation of radiative heat transfer in participating media of furnace combustion chamber, in this work, two radiation models have been applied: DTRM and DOM approximation with a finite volume approach. Both models are employed within the CFD software AVL FIRE™. These two models have different modelling approach in solving the radiative transfer equation (RTE) of participating media by their definition [5]. The DTRM model is based on the raytracing, which calculates the radiation intensity through the computational domain and has an utterly different modelling procedure from DOM featuring finite volume method [6]. In the pre-processing stage, the raytracing procedure is executed for each ray that is shot from the boundary face. The path through the computational domain is being calculated [7]. The input data of DTRM is a number of rays shot from the face, where for a greater number of rays, the more precise results will be obtained but will require more computational time [8]. For the DOM model, the input number of azimuthal and polar angles needs to be defined. After the spatial discretisation is conducted, the radiative heat transfer equation is calculated with transport equations for incident radiation in each spatial angle that represents one ordinate. Contributions of each ordinate are summed and added as input for calculation of the radiative source term in the energy conservation equation [9]. The authors of [10] show universality of DOM to be applied to a whole range of applications. The algorithm for obtaining ordinates directions and their spatial angles is described in [11]. Both modelling approaches (DTRM and DOM) are equally computationally demanding, and their accuracy is adjustable with input parameters [12]. Additionally, in this work, the absorptivity and emissivity are modelled as for isotropic media while the scattering phenomenon was not considered in observed simulations, since the soot participation in radiative heat transfer is well described by the grey-body model [13].

The recent research for optimising the combustion process by using CFD in combustion chambers showed that the application of radiative properties of the gas inside the steady system such as jet engine combustion chamber cannot be neglected [14]. The similar approach for investigating radiative heat transfer impact was used in the numerical modelling of heat transfer in strong swirl flow of furnaces [15]. Wang *et al.* [16], performed analysis of thermal efficiency with emphasis on the radiative impact calculated by DOM in reheating furnace. The AVL FIRE™ was already employed for steady calculations in biomass combustion in a rotary kiln in [17], where the similar framework is applied for the simulations in this work.

For the assessment of radiative heat transfer impact on temperature distribution in this work, IJmuiden furnace is selected for which dimensions and experimental data is available in [18]. The combustion process is modelled with steady combustion model (SCM) based on literature [19], where it was applied with and without heat transport by radiation. This SCM features fast convergence and steady solution of the combustion process and is applicable for the combustion process in oil-fired utility [20]. It is computationally less demanding

Jurić, F., *et al.*: Assessment of Radiative Heat Transfer Impact …
THERMAL SCIENCE: Year 2020, Vol. 24, No. 6A, pp. 3663-3672

3665

compared to the extended combustion models generally utilised in combustion systems like in [21]. A similar approach was applied for experimental oil furnace for emission predictions, but without radiation [22]. For the boundary conditions, diffusive opaque and inlet/outlet boundary conditions were applied for the calculation of incident radiation in directions that are oriented into the computational domain, based on the [23]. Similar approach was employed in [24], where the furnace gas temperature is predicted in reheating furnace with the P-1 radiation model. In [25], the estimation of radiative heat transfer in pulverised coal combustion is performed with the P-1, where the impact of particulate impact on incident radiation scattering is assumed.

Finally, this work aims to present the analysis of the radiative heat transfer in participating media with two different radiation models, DTRM and DOM in combination with SCM by employing CFD code AVL FIRE™ on an industrial furnace which includes the swirled combustion process. The performed validation of both radiative heat transfer models has shown that the presented modelling procedures are capable of predicting heat transport and can be used as a computationally fast tool that facilitates design and optimisation of industrial furnaces. The results with DTRM and DOM showed agreement in the validation against the experimental results. The results with DTRM and DOM showed agreement in the validation against the experimental results.

## Mathematical model

All simulations performed in this paper are described with Reynolds-Averaged Navier-Stokes equations. The Reynolds stress tensor was modelled by using the *k-ε* turbulence model, which details can be found in [26].

### *Combustion modelling*

The combustion process was modelled by SCM, which calculates a fast solution for the combustion process in oil-fired furnaces [20]. The SCM is based on empirical correlations for considering the impact of droplet evaporation, swirl motion, spray disintegration, chemistry kinetics on the oil combustion in an extended Arrhenius type expression. Additionally, SCM is applicable for the wide range of conventional oil flames. In SCM, the oil fuel is assumed in pre-mixed regime with the primary air-flow, due to consideration of the mixing time in combustion velocity. The model considers different reaction rate calculation:

$$\bar{r} = -\rho \frac{\partial \bar{y}_{fu}}{\partial t} = -k\rho \bar{y}_{fu} \bar{y}_{O_2} \tag{1}$$

where $k$ is the reaction rate constant, $\bar{y}_{fu}$ – the average fuel mass fraction, and $\bar{y}_{O_2}$ – the average oxygen mass fraction, which is considered in the eq. (1) if $\bar{y}_{O_2}$ is lower than 0.03. Constant $k$ could be characterized as a combustion velocity and is obtained from the following equation:

$$k = \frac{b}{t_{ei} + t_{ox}} \tag{2}$$

where the combustion velocity coefficient $b$ is considered 33 for the $\bar{y}_{O_2}$ lower than 0.03 and 1 for $\bar{y}_{O_2}$ higher than 0.03, due to the influence of enough oxygen. The denominator of the eq. (2) is called total time, and it consists of two terms. The first term is time of evaporation and induction, $t_{ei}$:

$$t_{ei} = A\exp\left(\frac{10^5}{RT}\right) + 0.45695d_{init}^{\ 2} \tag{3}$$

with $T$ as local temperature, R – the universal gas constant, and $d_{init}$ – the initial droplet diameter of value 0.3 mm. The second term is time of oxidation, which is calculated by following term:

$$t_{ox} = \frac{d_{init}^{\ 2}}{0.0032(T-T_0)-1.79} \tag{4}$$

In SCM fluid-flow is calculated only for one gaseous phase, which results that the evaporation process of inlet fuel is modelled inside the evaporation and induction time in eq. (3). Further description about evaporation time calculation can be found in literature [27]. This model gives good coverage of kinetic combustion for the lean region and for the burning of evaporated fuel in the region of disintegrated droplets. In SCM, the *b* is adjusted for different values of oxygen concentrations, which makes the reaction rate dependent on the availability of oxygen [20]. The mixing process of air and evaporated fuel in this work is amplified by the swirl motion of the primary inlet air. The inlet swirl velocity of primary air is defined by user-functions in the AVL FITE™, where the swirl ratio of 0.8 value around the *x*-axis is used. Additionally, this model is also suitable for calculating the flames formed in furnaces with the additional secondary inlet of air.

### Radiative heat transfer modelling

In this subsection, two different modelling approaches that are used in this paper for the calculation of radiative heat transfer are presented: DTRM and DOM.

#### Discrete transfer radiative method

The primary assumption of the DTRM is that a single ray can approximate the radiation leaving the surface element in a specific range of solid angles. Such an assumption of DTRM is made by employing raytracing, where the change of incident radiation of each ray is only followed until the ray hit the wall [28]. The shift in incident radiation along a ray path can be written:

$$\frac{dI}{ds} = \frac{a\sigma T^4}{\pi} - aI \tag{5}$$

where a change of incident radiation $I$ through path $s$ is equivalent to a difference of the emitted and absorbed incident radiation, described with the absorption coefficient $a$. For this research, the refractive index is assumed 1. The DTRM integrates eq. (5) along with a series of rays leaving the boundary faces. The incident radiation is defined as $I$ is calculated as [29]:

$$I = \frac{\sigma T^4}{\pi}\left[1-\exp(-as)\right] + I_0 e^{-as} \tag{6}$$

In the pre-processing, the raytracing paths are computed and saved before the start of fluid-flow calculations. An azimuthal angle from which the rays are shot is varied from 0 to $\pi$ and polar from 0 to $2\pi$. For each ray, length within each control volume that it intercepts is calculated and stored. All wall boundaries are taken as black and diffuse. Thus, the intensity leaving the wall is given:

$$I_{bnd} = \frac{\sigma T_w^{\ 4}}{\pi} \tag{7}$$

where $T_w$ is the wall temperature and $\sigma$ – the Stefan-Boltzmann constant. That means that the outgoing radiation flux is composed only of the directly emitting. The incident radiation at inlets and outlets leaves the calculation domain. Therefore, it is not reflected on inlet and outlet boundaries, and it is calculated:

$$I_{of} = \frac{\sigma T_{of}{}^4}{\pi} \tag{8}$$

where $T_{of}$ is the temperature of the outflow boundary. The incident radiation flux at the boundary element is then calculated as the sum of incident intensities for all rays. In participating media, the energy gain or loss in internal cells due to radiation is given through the radiation source term. The radiation source term is then inserted as source term of the enthalpy conversation equation. The overall energy gain or loss for a specific internal cell is calculated from the sum of all rays the contributions crossing the cell.

*Discrete ordinates method*

The radiation in participating media was also modelled by the DOM model featuring a finite volume approach. The radiative heat transfer in the DOM is based on solving RTE, which is consisting of two mechanisms: absorption and emission. Participating media absorbs the incoming radiation, which is then enhanced by the emission of the media in *j* direction:

$$\frac{dI_j}{ds_j} = -\left(a + \sigma_s\right)I_j + a\left(\frac{\sigma T^4}{\pi}\right) \tag{9}$$

where $I_j$ is the intensity of incident radiation in the *j* direction, $a$ – the absorption coefficient, and $s_j$ – the ordinate direction with its spatial angle $\Delta\Omega j$. Spatial angle discretization is defined as the ordinate direction $s^l$ is oriented perpendicular to its spatial angle. The eq. (9) has to be solved for each discretised spatial angle, but the minimal number is recommended to be eight [13]. When the intensity of incident radiation in each ordinate direction is obtained, the incident radiation is calculated:

$$G = \sum_{j=1}^{n} I_j \Delta\Omega_j \tag{10}$$

where *n* is the total number of control angles that is defined by discretisation of spatial angles. It can be noticed from eq. (10) that the incident radiation depends mainly on the temperature, where the interaction between the radiation heat transfer and the radiative power source is modelled:

$$S_{rad} = a\left(G - 4\sigma T^4\right) \tag{11}$$

The boundary conditions in this work are assumed as the diffusive walls and are calculated only for the ordinates that have an orientation in the computational mesh. Diffusive opaque walls are defined as [10]:

$$I_{bnd\,j} = \epsilon \frac{n_r}{\pi}\left(\sigma T^4\right) + \left(1 - \epsilon\right)\frac{\displaystyle\sum_{(s_j \cdot n_i)>0} I_j \left|n_i D_{ci}\right|}{\displaystyle\sum_{(s_j \cdot n_i)<0} n_i D_{ci}} \tag{12}$$

where $\epsilon$ is the wall emissivity and $D_{ci}$ – the auxiliary variable for solving orientations of spatial angles in regard to cell face orientation. For the calculation intensities of incident radiation in

3668

Jurić, F., *et al.*: Assessment of Radiative Heat Transfer Impact …
THERMAL SCIENCE: Year 2020, Vol. 24, No. 6A, pp. 3663-3672

eq. (9), the upwind differencing scheme (UDS) is applied. Convergence criterium is defined as the ratio of the difference between the new and old value of incident radiation divided by the old incident radiation value, and in the following simulations equals 0.001.

### Absorption coefficient modelling

Absorption coefficient in this work is modelled by implemented weighted sum of gray gases model (WSGGM) for grey gases, which is based on the $CO_2$ and $H_2O$ correlations in the literature [30]. The total absorption coefficient $a$ is defined:

$$a = -\frac{\ln(1-\varepsilon)}{s} \tag{13}$$

Emissivity $\varepsilon$ in eq. (13) is defined in eq. (14):

$$\varepsilon = \sum_{i=0}^{2} \alpha_i \left[1 - \exp\left(-a_i p s\right)\right] \tag{14}$$

where $\alpha_i$ is weight factor of the grey gas $i$, $a_i$ is its radiative absorption coefficient, $p$ – the partial pressures of the of $i^{th}$ grey gas. The weighting factors of grey gas $i$ are defined by the polynomial term for which the polynomial coefficients $b_{i,j}$ are tabulated:

$$\alpha_i = \sum_{j=0}^{3} b_{i,j} T^j \tag{15}$$

For $i$ equals zero, the transparent gas is assumed. The weight factor of transparent gas is defined as:

$$\alpha_0 = 1 - \sum_{i=0}^{2} \alpha_i \tag{16}$$

### Numerical setup

In fig. 1, the computational mesh with around 177 000 control volumes is generated, for which the mesh dependency test was performed on two finer meshes with the input cell size 66% and 50% of the initial cell size. Simulation performed on all three meshes showed flow, temperature and turbulence quantities with the relative deviation lower than 0.5%. For the mass conservation equation, the central differencing scheme (CDS) was employed. In contrast, for the turbulence, energy and volume fraction transport equations, the first order UDS was applied. For the momentum equation, a combination of CDS and UDS was proposed by introducing a blending factor of 0.5. The convergence of the solution was achieved when the normalised pressure residual reached values lower than $5 \times 10^{-4}$ also, momentum and energy residuals lower than $10^{-4}$. For turbulence, energy and volume fraction transport equations the first-order UDS was used, while for the continuity equation, the CDS was employed. For the momentum equation, the MINMOD Relaxed scheme was employed [20]. The convergence criteria were satisfied when normalised energy, momentum and pressure residuals reached a value lower than $10^{-4}$. For the DOM the RTE was solved each twentieth fluid-flow iterations. For the numerical simulations in this work crude oil fuel was modelled as a chemical compound with the average chemical formula $C_{13}H_{23}$, where the lower heating value is set to 41.1 $MJkg^{-1}$, and physical properties as density and viscosity are adopted from the AVL FIRE™ fuel database.
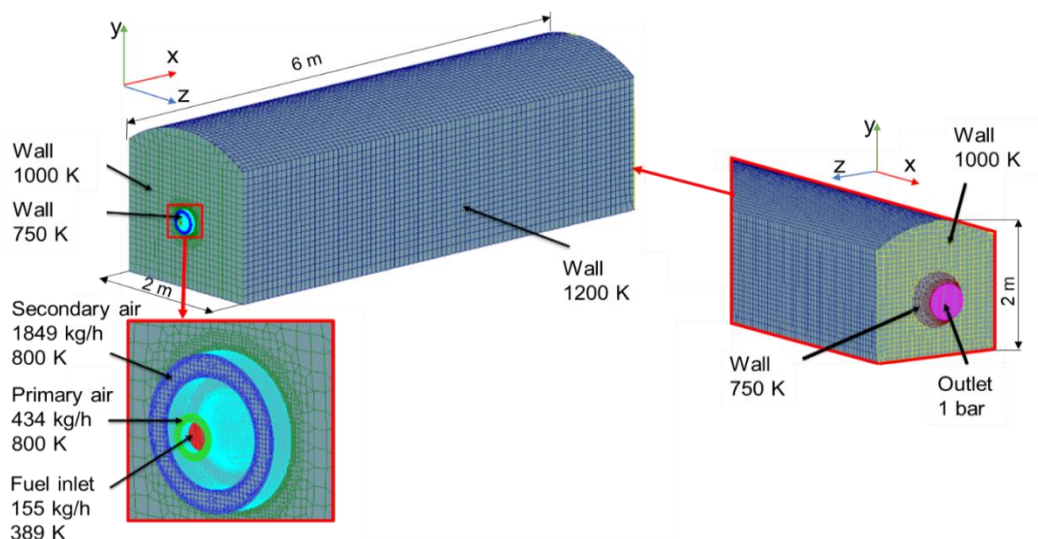
**Figure 1. Computational domain with the boundary conditions**

The boundary selections are shown in fig. 1, with the wall, inlet and outlet boundary conditions. The wall selections were defined as Dirichlet boundary condition of fixed temperature, and the air and fuel entrainment were prescribed with a constant temperature mass-flow. In the following case, all wall boundaries are set with an emissivity value 1. At the outlet selection, the static pressure was prescribed. Characteristic for the IJmuiden furnace is the secondary air with four times larger mass-flow. Spray parameters are considered inside the combustion model, which resulted in deficient computational time. That is precisely why this model is chosen for the combustion modelling in the furnace, to have an emphasis on the radiative heat transfer. For the DTRM raytracing, local hemisphere discretization was achieved with discretising boundary hemisphere with two polar angles and eight azimuthal angles. Thermal boundary under-relaxation factor was set to 0.5, and the tolerance was set to 0.01.
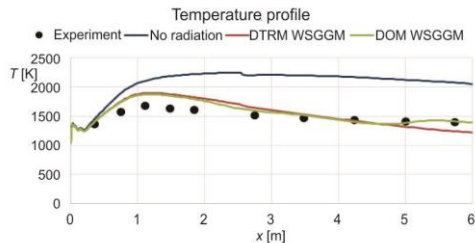
## Results

In this section, critical specific objectives, the significant findings, and the most significant conclusions of the paper are presented. The presented temperature results for the verification furnace case are calculated for the steady-state, where the convergence of results is achieved after approximately 3000 fluid-flow iterations.

Figure 2 shows the results at the line connecting the centre of the inlet and centre of the outlet. The black dots represent experimental temperature measurements that are used for validation of radiation models. The blue curve shows results without radiation, that indicate overprediction of temperature results, and pronounced radiative gas emission losses in the furnace. The orange curve shows results obtained with the DTRM, while the green curve represents the results obtained with the DOM. The main difference between DTRM and DOM results is visible at the outlet of the domain, and it can be attributed to the outlet geometry that makes uncertainty raytracing. Furthermore, the better trend with calculation without radiation is achieved with the DTRM, which can be assign to lack of rays that hit the cells in the near outlet region.

Figure 3 shows measured distributions of unidirectional radiation intensity through a steady-state oil flame, where the results with radiation are showed against experimental re-

3670

Jurić, F., *et al.*: Assessment of Radiative Heat Transfer Impact …
THERMAL SCIENCE: Year 2020, Vol. 24, No. 6A, pp. 3663-3672



**Figure 2. Temperature profile comparison between experimental data, combustion model without radiation and with DTRM and with DOM**
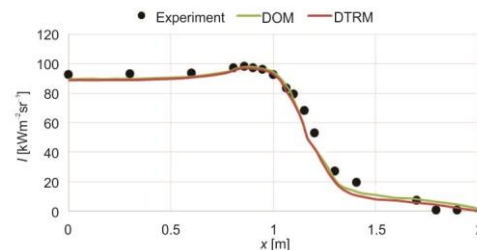


**Figure 3. Comparison between calculated and measured distributions of unidirectional radiation intensity through a steady-state oil flame**

sults. Both models show good agreement with experimental results and with their trend. The DOM results have slightly overprediction compare to the DTRM results during the whole region, which is especially pronounced between 1.5 m and 2 m of flame. The difference in these results is the outcome from the model equations, that differently calculate the gas emission in the flame cells.

   In fig. 4, at the top, the temperature field results are shown for the case where the radiative heat transfer was not considered. The colder fuel region is visible near the inlet due to the lower air and fuel temperature. Inside the combustion chamber after the spray region, the practically uniform temperature field is achieved with the temperature of around 2200 K.

   The DTRM and DOM results show a good agreement in a temperature distribution inside the combustion chamber. Difference between results with included radiative heat transfer and without radiation is in the near-wall temperatures and around the inlet, due to no presence of gas emissions in heat transfer. That can be attributed to the low temperature region of the injected fuel and the high emissivity of the media near the walls. The lower mean temperature obtained in the simulations with included DTRM has a slightly broader and shorter flame region, which is especially visible in the area near the outlet, which is also evident in fig. 2 diagram. The computational time of the showed results is four times more expensive for DTRM case compared to the case without calculation of the radiative heat transfer in participating media. The DTRM pre-processing of raytracing contributes most to that difference, which needs to be calculated only once before the start of the first calculation. Additional computational demand of DTRM is also obtained due to low CPU parallelisation potential, where the communication between CPU is aggravated by waiting for raytracing information, unlike the DOM where the parallelisation is faster.
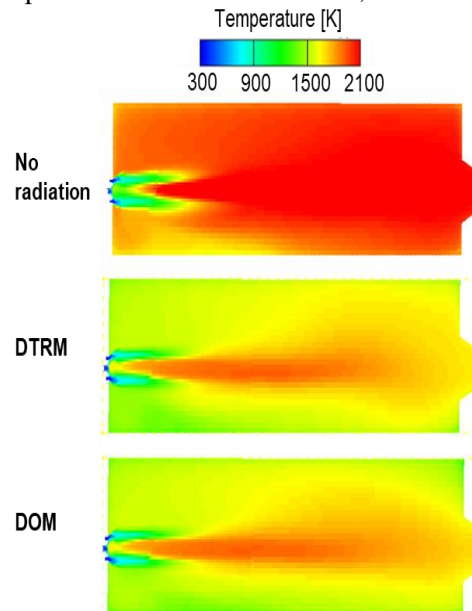


**Figure 4. Temperature field results at the symmetry plane of the computational domain**

Jurić, F., *et al.*: Assessment of Radiative Heat Transfer Impact …
THERMAL SCIENCE: Year 2020, Vol. 24, No. 6A, pp. 3663-3672

3671

## Conclusion

The radiative heat transfer analysis in CFD of the steady combustion process provides a valuable tool that can be used to investigate more accurate and better understand the combustion process. The feasibility of DTRM and DOM radiative heat transfer models in the AVL FIRE™ code is examined, where the focus is on their comparison and application in combination with the combustion process inside a furnace combustion chamber. Simulations performed with SCM are presented for three cases: without radiative heat transfer, with radiation calculated by DTRM, and with radiation calculated by implemented DOM. The comparison of the CPU execution time showed that the calculation with DTRM is 3.8 times, and with DOM 2.3 times more time consuming than the case without calculation of the radiative heat transfer in participating media. The validation results showed good agreement with the experimental data with a better prediction of DOM model in the temperature trend near furnace outlet, which can be attributed to the shortcomings of DTRM raytracing in the near outlet region. The comparison of temperature distribution shows that the temperature field predicted with the DOM approach has a good agreement with the DTRM results, where a similar trend to the simulation without radiation is achieved. Furthermore, the main difference between DTRM and DOM results is visible at the outlet of the furnace, where the outlet geometry impacts the DTRM raytracing uncertainty. While for the DOM calculation, the incident radiation is calculated in every cell, which results in a better agreement with the experimental temperature profile along with the furnace. The calculations with the DTRM and DOM model are compared with the simulation without calculating radiative heat transfer, where approximately 25% higher temperatures are reached. Finally, it can be stated that the presented method with DTRM and DOM models can serve as a solution for a swift investigation of the radiative heat transfer in participating media of real industrial furnaces.

## Acknowledgment

## References

[1] Ren, T., *et al.*, Machine Learning Applied to Retrieval of Temperature and Concentration Distributions From Infrared Emission Measurements, *Appl. Energy*, *252* (2019), Oct., pp. 1-15
[2] Modest, M. F., Haworth, D. C., Radiative Heat Transfer in High-Pressure Combustion Systems, in: *Springer Briefs in Applied Sciences and Technology*, Springer, New York, USA, 2016, pp. 137-148
[3] Vujanović, M., *et al.*, Sustainable Energy Technologies and Environmental Impacts of Energy Systems, *Appl. Energy*, *256* (2019), Dec., pp. 1-11
[4] Maginot, P. G., *et al.*, High-Order Solution Methods for Grey Discrete Ordinates Thermal Radiative Transfer, *J. Comput. Phys.*, *327* (2016), C, pp. 719-746
[5] Mishra, S. C., *et al.*, Development and Comparison of the DTM, the DOM and the FVM Formulations for the Short-Pulse Laser Ttransport Through a Participating Medium, *Int. J. Heat Mass Transf.*, *49* (2006), 11-12, pp. 1820-1832
[6] Coelho, P. J., Advances in the Discrete Ordinates and Finite Volume Methods for the Solution of Radiative Heat Transfer Problems in Participating Media, *J Quant Spectrosc Radiat Transf*, *145* (2014), pp. 121-146
[7] Honus, S., Juchelková, D., Mathematical Models of Combustion, Convection and Heat Transfer in Experimental Thermic Device and Verification, *Teh. Vjesn.*, *21* (2014), 1, pp. 115-122

3672

Jurić, F., *et al.*: Assessment of Radiative Heat Transfer Impact …
THERMAL SCIENCE: Year 2020, Vol. 24, No. 6A, pp. 3663-3672

[8]   Coelho, P. J., Carvalho, M. G., A Conservative Formulation of the Discrete Transfer Method, *J. Heat Transfer*, *119* (1997), 1, pp. 118-128

[9]   Chai, J. C., *et al.*, Finite Volume Method for Radiation Heat Transfer, *J. Thermophys Heat Trans.*, *8* (1994), 3, pp. 419-425

[10]  Coelho, P. J., Advances in the Discrete Ordinates and Finite Volume Methods for the Solution of Radiative Heat Transfer Problems in Participating Media, *J Quant Spectrosc Radiat Transf*, *145* (2014), Sept., pp. 121-146

[11]  Mishra, S. C., Roy, H. K., Solving Transient Conduction and Radiation Heat Transfer Problems Using the Lattice Boltzmann Method and the Finite Volume Method, *Jou. Comput. Phys.*, *223* (2007), 1, pp. 89-107

[12]  Coelho, P. J., Radiative Transfer in Combustion Systems, in: *Handbook of Thermal Science and Engineering*, Springer, New York, USA, 2017, pp. 1173-1199

[13]  Modest, M. F., *Radiative Heat Transfer Elsevier* (3rd ed.). Elsevier, Amsterdam, The Netherlands, 2013

[14]  Tulwin, T., A Coupled Numerical Heat Transfer in the Transient Multicycle CFD Aircraft Engine Model, *Procedia Eng.*, *157* (2016), Dec., pp. 255-263

[15]  Silva, J., *et al.*, CFD Modeling of Combustion in Biomass Furnace, *Energy Procedia*, *120* (2017), Aug., pp. 665-672

[16]  Wang, J., *et al.*, Analysis of Slab Heating Characteristics in a Reheating Furnace, *Energy Convers. Manag.*, *149* (2017), Oct., pp. 928-936

[17]  Mikulčić, H., *et al.*, Sustainability Through Combined Development of Energy, Water and Environment Systems, *J. Clean. Prod.*, *251* (2020), Apr., pp. 1-35

[18]  Johnson, T. R., Beer, J. M., Radiative Heat Transfer in Furnaces: Further Development of the Zone Method of Analysis, *Proceedings of Symposium (International) on Combustion*, *14* (1973), 1, pp. 639-649

[19]  Vujanović, M., *et al.*, User Function Approach in Modelling of Nitrogen Oxides in Commercial CFD Code FIRE, *Proceedings*, ECCOMAS Thematic Conference on Computational Combustion, Lisbon, Portugal, 2004, pp.1-8

[20]  ***, AVL AST GmbH, FIRE Documentation v2019, Graz, Austria, 2019

[21]  Jurić, F., *et al.*, Experimental and Numerical Investigation of Injection Timing and Rail Pressure Impact on Combustion Characteristics of a Diesel Engine, *Energy Convers. Manag.*, *185* (2019), Apr., pp. 730-739

[22]  Jozsa, V., Kun-Balog, A., Stability and Emission Analysis of Crude Rapeseed Oil Combustion, *Fuel Process. Technol.*, *156* (2017), Nov., pp. 204-210

[23]  Baburić, M., *et al.*, Application of the Conservative Discrete Transfer Radiation Method to a Furnace with Complex Geometry, *Numerical Heat Transfer, Part A: Applications*, *48* (2005), 4, pp. 297-313

[24]  Qi, F., *et al.*, Numerical Study on Characteristics of Combustion and Pollutant Formation in a Reheating Furnace, *Thermal Science*, *22* (2018), 5, pp. 2103-2112

[25]  Filkoski, R., *et al.*, Optimization of Pulverised Coal Combustion by Means of CFD/CTA Modeling, *Thermal Science*, *10* (2006), 3, pp. 161-179

[26]  Honus, S., *et al.*, Verifying the Prediction Result Reliability Using $k$-$\varepsilon$, Eddy Dissipation, and Discrete Transfer Models Applied on Methane Combustion Using a Prototype Low-Pressure Burner, *Adv. Sci. Technol. Res. J.*, *11* (2017), 4, pp. 252-259

[27]  Csemany, D., Jozsa, V., Fuel Evaporation in an Atmospheric Premixed Burner: Sensitivity Analysis and Spray Vaporization, *Processes*, *5* (2017), 80, pp. 1-16

[28]  Abraham, J., Magi, V., Application of the Discrete Ordinates Method to Compute Radiant Heat Loss in a Diesel Engine, *Numerical Heat Transfer, Part A: Applications*, *31* (1997), 6, pp. 597-610

[29]  Hosseini Sarvari, S. M., Solution of Multi-Dimensional Radiative Heat Transfer in Graded Index Media Using the Discrete Transfer Method, *Int. J. Heat Mass Transf.*, *112* (2017), Sept., pp. 1098-1112

[30]  Dorigon, L. J., *et al.*, WSGG Correlations Based on HITEMP2010 for Computation of Thermal Radiation in Non-Isothermal, Non-Homogeneous $H_2O/CO_2$ Mixtures, *Int. J. Heat Mass Transf.*, *64* (2013), Sept., pp. 863-873